

Gigabit DSL

Bin Lee, John M. Cioffi and Mehdi Mohseni

Department of Electrical Engineering

Stanford University

Stanford, CA, 94305

Email: {binlee, cioffi, mmohseni}@stanford.edu

Abstract— This paper applies multiple input multiple output (MIMO) transmission methods to multi-wire communication systems. Using channel matrices generated from a binder MIMO channel model, a performance assessment of digital subscriber line technology based on MIMO transmission methods finds practically achievable data rates of over one gigabit per second symmetric data rate over 4 twisted pairs (category 3) for 300 meter range are possible. Similar results are also obtained for a “quad” cable. To achieve the data rate readily, this paper proposes that the source and load be excited using common mode.

Index Terms— MIMO systems, Twisted pair cables, Digital subscriber line, GDSL

I. INTRODUCTION

Gigabit DSL (digital subscriber line) services are technically feasible and tease the imagination of telephone company service providers. Such speeds well in excess of present DSL data rates necessitate a number of topological and signal-processing challenges. Fiber to within 300 meters of the subscriber is presumed, and then the fundamental practical data-carrying limits of 2-4 copper twisted pairs in the remaining final drop segment to the customer using vectored MIMO technology will exceed 1 Gbps symmetric transmission. This paper evaluates such situations and details the basic architecture and structure necessary to implement symmetric gigabit per second DSLs or GDSL.

The usual adversary of DSL systems, crosstalk, becomes an enhancement to capacity in the final drop segment where typically 2-6 twisted-pair connect a residence or business with the so-called “service terminal” or “pedestal.” While extra copper does not usually exist to connect all customers’ 2-6 wires back to the central office, extra copper does often exist in the drop segment. Since fiber presumably will connect the pedestal back to the central office, the need for spare copper capacity in that to-central-office segment is no longer necessary. Thus, all the wires in the drop segment may be exploited and used for best achievable data rate to the customer. Coordination of the signals on the final drop with good design practices known as vectoring and bonding allow the entire drop binder of 2-6 wires to be viewed as a single transmission path that can have enormous latent capacity.

Modeling of such a binder is addressed in an earlier paper [3], and Section 2 of this paper investigates the key elements of the 300 meter (or less) drop segment in deriving a reasonable model for evaluation of data-carrying capability. Such modeling is often known as Multiple Input Multiple Output (MIMO). Section 2 also addresses the potential non-crosstalk noises and assumptions that are made in this study of best achievable data rates in the binder segment. Having established a viable model for the drop binder, Section 3 proposes well-known vector transmission methods to cancel crosstalk, and even to exploit, far end crosstalk (FEXT) [1]-[2]. Vectored receivers also allow significant reduction of remaining non-crosstalk noises, as is discussed in Section 3. Section 4 then uses specific line parameters to determine that indeed symmetric speeds in excess of 1 Gbps are readily feasible up to at least 300 meters of drop binder on no more than 4 twisted pairs.

II. BINDER MIMO CHANNEL

For a practical multi-twisted pair cable system, the MIMO channel response function can be written as (see [1], Chapter 11 and also the ANSI MIMO model in [5]):

$$\mathbf{Y} = \mathbf{H}\mathbf{X} + \mathbf{N} \quad (1)$$

In (1), \mathbf{Y} is an output column vector whose components are the outputs of the individual transmission lines and \mathbf{X} is an input column vector. The MIMO channel transfer matrix \mathbf{H} is typically constant (or varies slowly with temperature) if the inputs are synchronized as would be the case in a MIMO GDSL system. \mathbf{N} is non-crosstalk noise that includes thermal noise, radio frequency interference and sometimes impulse noise. In DSL systems, (1) is very representative of a vectored DMT (discrete multi-tone) systems that have been standardized for most DSL transmission. In addition to clock synchronization, symbol synchronization is achieved through what is known as “digital duplexing” (see [1], Chapter 3). In this case, Equation (1) holds independently for each “tone” (frequency sub-channel) of a DMT system. A tone index is not used in (1) to simplify notation, but is presumed. Crosstalk is included in \mathbf{H} , so for instance for 4 lines, each tone has a \mathbf{H} matrix that models the crosstalk on that tone between the lines. Because of the common symbol clock, there is no interference nor crosstalk between tones of different frequency indices [1].

The binder MIMO channel model of [3] and [5] provides a method to calculate \mathbf{H} from system physical parameters under a variety of excitation and load conditions and for various assumptions of twist lengths, imperfections, and twisted-pair spacings. The model treats cable as cascades of segments, and each segment can be described by time-invariant transmission-line equations:

$$\begin{aligned} -\frac{d\mathbf{V}}{dz} &= (\mathbf{R} + j\omega\mathbf{L}) \cdot \mathbf{I} \\ -\frac{d\mathbf{I}}{dz} &= (\mathbf{G} + j\omega\mathbf{C}) \cdot \mathbf{V} \end{aligned} \quad (2)$$

Due to twisting of cables and various cable geometric imperfections, **RLCG** matrices are position dependent and can be computed using basic electromagnetic methods. The transmission line equations can be solved analytically for each segment, and input-output relation for a complete cable can be calculated by considering cascades of segments. To get a channel transfer matrix for a complete system,

load and excitation conditions need to be considered. Fig. 1(a) shows the typically encountered differential excitation configuration for a 4 twisted pair cable, where source and load impedances are individually applied to each pair of conductor wires. With differential excitation, a line transfer function can be defined for each pair and FEXT can be defined between any two different pairs. Fig. 1(b) shows a common-mode or “split-pair” excitation configuration, where all 8 wires in 4 pairs are treated equally and one wire is chosen as common reference [3]. Here a characteristic impedance matrix \mathbf{Z}_0 can describe cable binder, \mathbf{Z}_0 is usually frequency as well as position dependent. Under this configuration, there is some freedom to choose load impedance matrices \mathbf{Z}_L . One practical choice is to select \mathbf{Z}_L matrix matching to \mathbf{Z}_0 ; another choice is to select \mathbf{Z}_L as diagonal matrices. (On source \mathbf{Z}_S , a designer can create an analog source with as close to zero internal resistance on each of the 7 excitation paths to not lose energy in the source resistance.) In either the diagonal or matched case, the capacity of the binder is significantly elevated by exploiting the “split-pair” modes between the lines in addition to the differential modes that are normally excited.¹ This capacity increase is due to the high crosstalk terms in channel matrix for “split mode”, a numerical example to illustrate such characteristics is in section 4.

Under both differential and common-mode excitations, a MIMO channel matrix can be defined for the channel. If \mathbf{X} is an input voltage vector, and \mathbf{Y} is an output voltage vector, then the channel matrix \mathbf{H} describe the voltage input-output relationship:

$$\mathbf{V}_L = \mathbf{H} \cdot \mathbf{V}_S, \text{ where } \mathbf{V}_L = \mathbf{Y} \text{ is output voltage vector, } \mathbf{V}_S = \mathbf{X} \text{ is input voltage vector} \quad (3)$$

\mathbf{H} can be described by a 7x7 matrix for 4 pairs at any given frequency. In additional to this 7x7 channel matrix, under the differential excitation, a simplified channel matrix can be defined by considering direct transfer function of pairs and far end crosstalk. For the 4 twisted pairs shown in Fig.1(a), a *simplified differential* 4x4 channel matrix can be defined as [3]:

$$\mathbf{H}_{sd} = \begin{bmatrix} T1 & Fext_12 & Fext_13 & Fext_14 \\ Fext_21 & T2 & Fext_23 & Fext_24 \\ Fext_31 & Fext_32 & T3 & Fext_34 \\ Fext_41 & Fext_42 & Fext_43 & T4 \end{bmatrix} \quad (4)$$

¹ When using split pair excitations, caution must be ensured to “silence” (reduce PSD significantly) in the known amateur radio bands that overlap the DC to 30 MHz bandwidth that we use for GDSL simulations in this paper. Such reduction has relatively minor effect in reducing the overall data rate.

where pair-wise direct transfer functions are on diagonal positions of the matrix, and FEXT is on off-diagonal positions of the matrix. Both 7x7 and 4x4 channel matrices can be calculated using the binder MIMO channel model [3]. After the frequency-dependent channel matrix \mathbf{H} (or \mathbf{H}_{sd}) is obtained, digitally duplexed and vector-synchronized discrete multi-tone (DMT) based DSL communication methods (see [1]) can be applied to the channel for each tone.

III. VECTOR TRANSMISSION METHOD AND TRANSCEIVER ARCHITECTURE

This section presents vector transmission method to estimate the data rate for a channel and system architecture to achieve the targeted data rate. For the proposed GDSL system of this paper, coordination of both transmitter and receiver is used, and data rate can be calculated in the following procedure: \mathbf{H} is computed as a function of frequency, $\mathbf{H}(f)$. (Methods presented in this section apply to both \mathbf{H} and \mathbf{H}_{sd} , without loss of generality, the symbol \mathbf{H} is used to represent a channel matrix.) For any tone frequency $f = n \cdot \Delta f$, $n = 1, \dots, N_{sc}$ where N_{sc} is the maximum number of tones, Δf is tone width. The singular values of $\mathbf{H}(f = n \cdot \Delta f)$ can be found for each and every tone through singular value decomposition (SVD) as

$$\mathbf{H}(f) = \mathbf{U}(f) \cdot \mathbf{S}(f) \cdot \mathbf{V}^+(f) \quad (5)$$

where $\mathbf{S}(f) = \text{diag}(\lambda_1, \dots, \lambda_L)$, and typically L is the rank of $\mathbf{H}(f)$. The corresponding “subchannel SNR’s” can be computed:

$$g_{l,n} = g_l(f = n \cdot \Delta f) = \frac{\lambda_{l,n}^2}{\sigma^2} \quad (6)$$

where σ includes all noises but crosstalk². Execution of rate adaptive water-filling algorithm over $g_{l,n}$ with known gap Γ subject to a total energy constraint will produce the achievable data rate b [4]

$$b = \sum_{l=1}^L \sum_{n=1}^N \frac{1}{2} \log_2 \left(1 + \frac{\varepsilon_{l,n} \cdot g_{l,n}}{\Gamma} \right) \quad \text{where } \varepsilon_{total} = \sum_{l=1}^L \sum_{n=1}^N \varepsilon_{l,n} \text{ is fixed.} \quad (7)$$

Practical systems to achieve the targeted data rate predicted by above method can be implemented using

² If the other noise is stationary but not “white” or flat across all frequencies and users, one has a spatial noise correlation matrix R_{NN} at each frequency. Then a standard noise whitening matrix transformation (transform \mathbf{H} to $R_{NN}^{-1/2} \cdot \mathbf{H}$) occurs at each frequency and noise can then be further assumed to be white.

MIMO based DMT methods. The system architecture for MIMO based DMT system is similar to a usual DMT system used in DSL ([1], [4]). Using SVD in eq(4), the matrix channel in (1) can be reduced to a set of parallel scalar channels [4]:

$$\mathbf{Y} = \mathbf{H}\mathbf{X} + \mathbf{N} = \mathbf{U} \cdot \mathbf{S} \cdot \mathbf{V}^+ \cdot \mathbf{X} + \mathbf{N}, \text{ where } \mathbf{U}, \mathbf{V} \text{ are unitary matrices, } \mathbf{U}\mathbf{U}^+ = \mathbf{I}, \mathbf{V}\mathbf{V}^+ = \mathbf{I} \quad (8)$$

$$\mathbf{U}^+ \mathbf{Y} = \tilde{\mathbf{Y}} = \mathbf{S} \cdot \tilde{\mathbf{X}} + \tilde{\mathbf{N}}, \text{ where } \mathbf{S}(f) = \text{diag}(\lambda_1, \dots, \lambda_L), \tilde{\mathbf{X}} = \mathbf{V}^+ \mathbf{X} \quad (9)$$

$$\tilde{y}_l = \lambda_l \cdot \tilde{x}_l + \tilde{n}_l, 1 \leq l \leq L \quad (10)$$

Eq(10) characterizes a set of scalar channels. These scalar channels are independent of each other, thus usual DMT based transmission architecture can be directly applied to each scalar channel. Furthermore, the complexity of the MIMO based DMT system would be only slightly increased over L independent DMT systems. This is because the only additional complexity comes from conversion between $\tilde{\mathbf{X}}$ and \mathbf{X} , between $\tilde{\mathbf{Y}}$ and \mathbf{Y} in eq(9), these conversions can be implemented in matrix multiplications. Fig.2 shows DMT system architecture for one scalar channel in frequency domain (matrix multiplications required for the conversions are not shown in the figure). In the figure, N is number of tone, m_i represent modulation function for each tone, f_i^* is match filter for each tone, $0 \leq i \leq (N-1)$.

IV. NUMERICAL EXAMPLES

This section contains two numerical examples: one is to illustrate the channel characteristics of a binder; another is to illustrate system achievable data rate for 4 twisted pairs over short cable length. Fig.3 compares the magnitude of a channel matrix of the differential mode vs. that of the “split mode”. Here, to reduce the complexity of drawing, two instead of four twisted pairs are used. Twisted pairs are 24 American wire gauge(AWG), with twist rates of 3.8 and 4.5 inch. Cable is 300-meter long and average distance between pair centers is 1.7 mm. The channel matrices are calculated using methods outlined in Section 2. At any given frequency, channel matrix \mathbf{H} is a 3x3 matrix. The figure plots each element of \mathbf{H} against frequency. Fig. 3(a) is for the differential mode, here R_s and R_l for each pair is 100 Ohm. Fig. 3(b) is for the “split mode”, here $\mathbf{Z}_s = \text{diag}(100, 100, 100)$ Ohm, \mathbf{Z}_L is matrix matched to binder ($\mathbf{Z}_L = \mathbf{Z}_0$). The figure shows that crosstalk terms for “split mode” is higher than “differential

mode”. Even though the plot is for the specific set of cable parameters, crosstalk terms for “split mode” are larger is a general property, holding for other cable parameters. These larger crosstalk terms are responsible for higher data rate for “split mode” in the next example.

The next example uses methods in Section 2 to obtain channel matrix and uses methods in Section 3 to calculate system achievable data rate. In this application, the aggregate data rate of 4 twisted pairs for lengths up to 300-meters is calculated. The cable is 24AWG and assumed to be tightly bounded. Twist rates are: 3.5, 4.6, 4.4, and 4.2 inches. To calculate symmetric data rate, upstream and downstream data rates are held equal. Total data rate is calculated for all tones and is divided by 2 to get upstream and downstream data rates; 8192 tones and tone spacing of 4.3125 kHz are used. Additional parameters used are: 3.8 dB coding gain, 6 dB system margin, 10^{-7} targeted bit error rate, -140 dBm background noise and 10 dBm transmission power per line (total power for the system is $10 + 10 \cdot \log_{10}(4) = 16$ dBm). The aggregate 4-line data rate is calculated for following source-load configurations: For differential excitation, each pair is differentially terminated with a 100 Ohm impedance, a data rate is calculated for both the 7x7 channel and *simplified differential* 4x4 channel matrices. For the common-mode MIMO excitation, the source is chosen to be individually excited (\mathbf{Z}_S is a diagonal matrix); two different load configurations are used: matrix matching ($\mathbf{Z}_L = \mathbf{Z}_0$) or diagonal matrix \mathbf{Z}_L . When \mathbf{Z}_S and \mathbf{Z}_L are diagonal matrices, the diagonal elements of these matrices are chosen to be 100 Ohms. Fig.4 shows the achievable data rate for these source-load configurations. A few observations derive from the figure. First, the data rate for a 7x7 matrix channel is higher than that of a 4x4 matrix channel, which is expected from MIMO theory. Second, a common-mode channel has a higher data rate than a differential-mode channel; this can be seen by comparing the data rate of the 7x7 channel with the differential load vs. the diagonal matrix load. Third, the data rate for a diagonal matrix load is comparable to that of a matrix-matching load. Given the fact that a diagonal matrix load is simpler to implement than a matrix matching load, this result suggests that a diagonal matrix load can be chosen in practical designs. Finally and most importantly, symmetric (both upstream and downstream) gigabit/s data rate is shown achievable for the system, which proves that gigabit DSL (GDLS) is possible for 300 meter with 4 twisted pairs using frequency band between 0 – 35 MHz.

Other simulations show that comparable data rate can be obtained for “quad” cable (2 basic quads, 8 wires total) with same frequency bands. Additionally, more simulations show that data rate is insensitive to both cable geometric parameters and cable imperfections. In the case of twisted-pair cable, data rate is shown to be insensitive of cable twist rates, average distances between pairs, relative position of pairs and various imperfections. In contrast, cable geometric parameters and imperfections have been shown to be critical for modeling crosstalk under differential excitations ([3], [5]). Two reasons account for the insensitivity of data rate vs. geometric parameters: a) when load is matrix matching to a binder or when load is a diagonal matrix, direct current paths exist between wires, therefore crosstalk between wires is almost independent of geometric parameters. b) when differential excitation is used, even though crosstalk is sensitive to geometric parameters, crosstalk is completely cancelled by vector transmission method, thus does not affect the data rate.

V. CONCLUSION

This paper shows that by applying MIMO transmission and discrete multi-tone techniques, symmetric data rates in excess of one gigabit per second or GDSL is possible for 4 twisted pairs over 300 meter cable length. It also shows that common mode matrix channel can achieve higher data rate over differential model matrix channel for same cable binder. The concepts of matrix channel, MIMO transmission as well matrix load proposed in this paper might also be applied to gigabit or 10 gigabit Ethernet over other categories of copper twisted-pair channels, and significant performance increase could be expected also in those applications.

REFERENCES

- [1] T. Starr, M. Sorbara, J. M. Cioffi, P. J. Silverman, DSL Advances. Prentice Hall, 2003
- [2] G. Ginis, J. M. Cioffi, “Vectored transmission for digital subscriber line Systems”, *IEEE J. Select. Areas Commun.*, VOL. 20, NO. 5, JUNE 2002, pp.1085-1104
- [3] B. Lee, K. Seong, Y. Kim, M. Mohseni, M. H. Brady, J. M. Cioffi, “Binder MIMO Channel”, submitted.
- [4] J. M. Cioffi, EE379C course note, <http://www.stanford.edu/class/ee379c>, chapter 4
- [5] ANSI Dynamic Spectrum Report Draft, T1E1.4/2003-RB, May 2004.

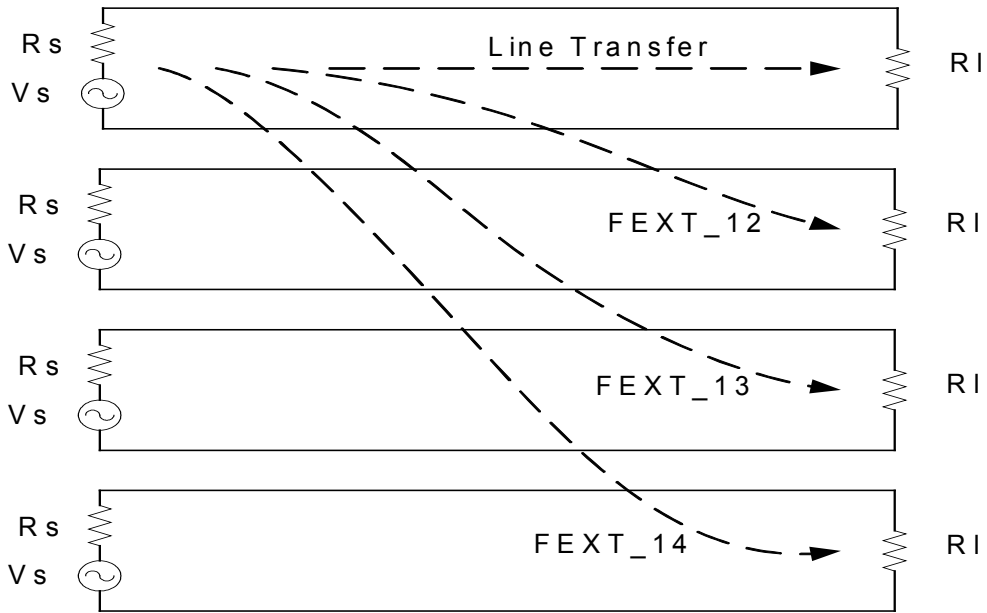


Figure 1(a), Differentially Excited MIMO Channel, a 7x7 or 4x4 channel can be defined for it

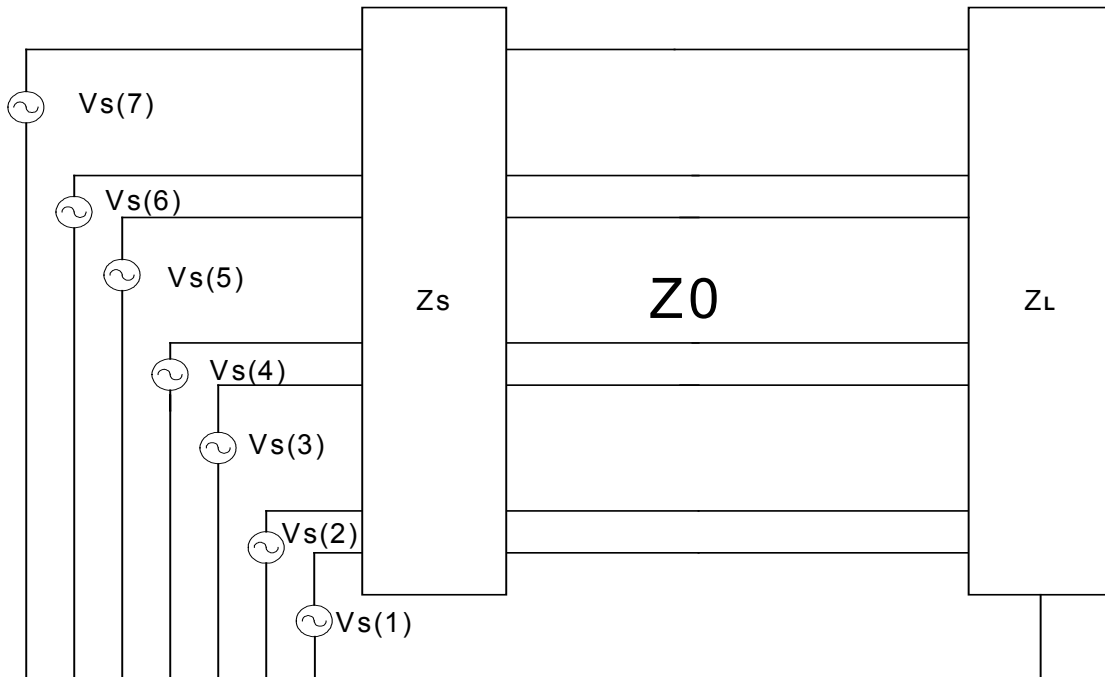


Figure 1(b), Common Mode MIMO Channel

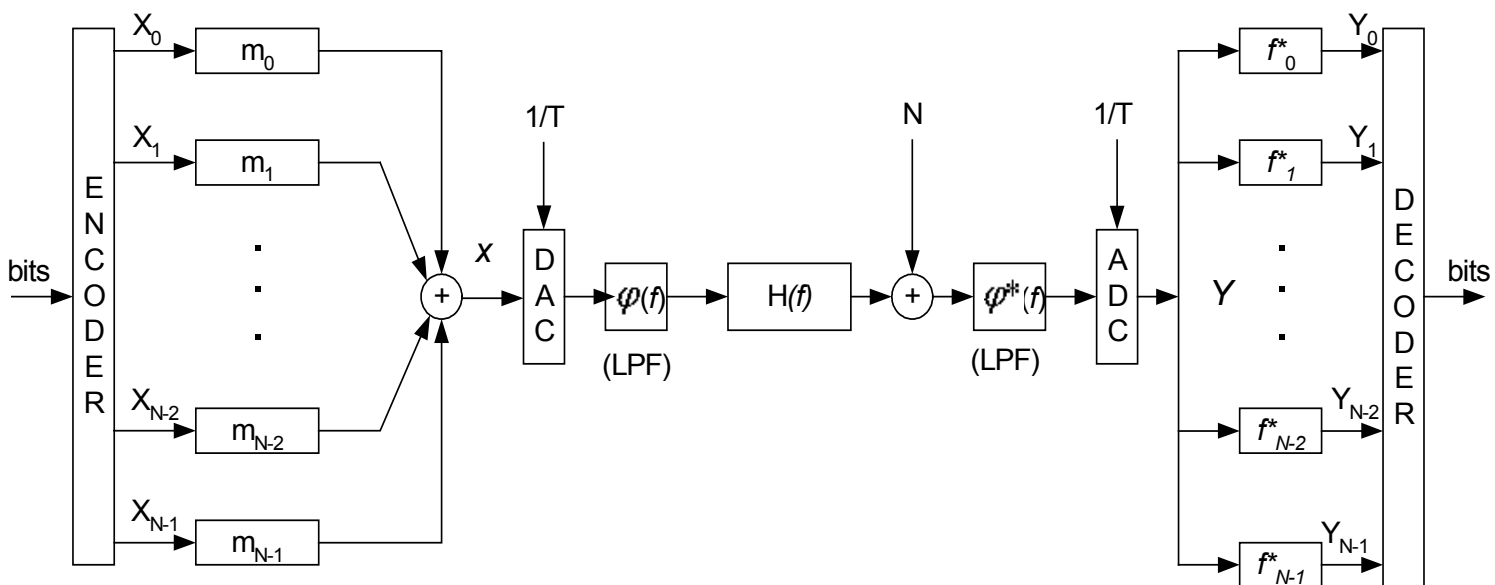


Figure 2, DMT System for one scalar channel, $Y = \tilde{y}_l, H(f) = \lambda_l(f), X = \tilde{x}_l, 1 \leq l \leq L$

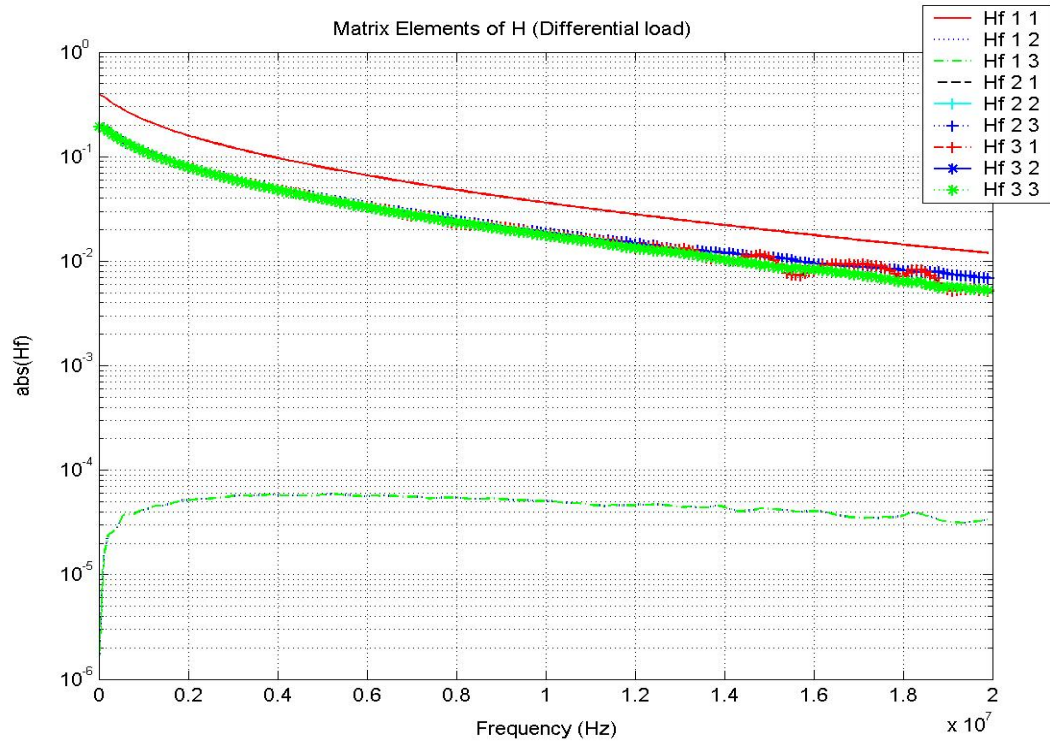


Figure 3(a), Channel Matrix for Two Twisted Pairs Under Differential Load
 Due to existing of symmetry in this simulation, $H(1, 2) \approx -H(1, 3)$,
 $H(2, 1) \approx H(3, 1)$, $H(2, 2) \approx H(2, 3)$, $H(3, 2) \approx -H(3, 3)$

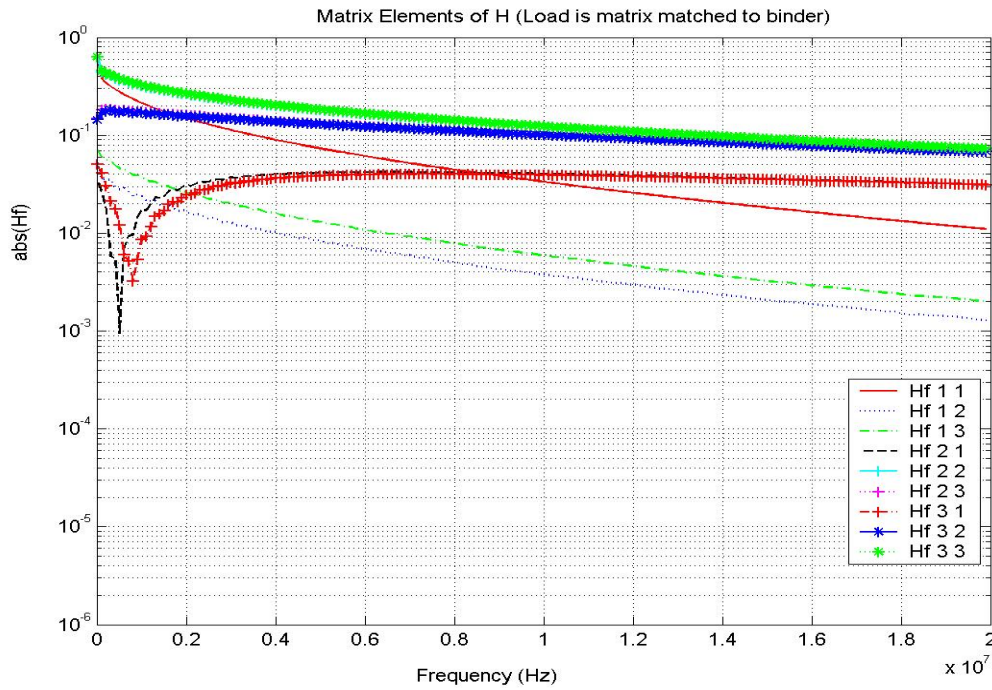


Figure 3(b), Channel Matrix for Two Twisted Pairs, Matrix Matched Load
 Due to existing of symmetry in this simulation, $H(2, 2) \approx H(3, 3)$,
 $H(2, 3) \approx H(3, 2)$

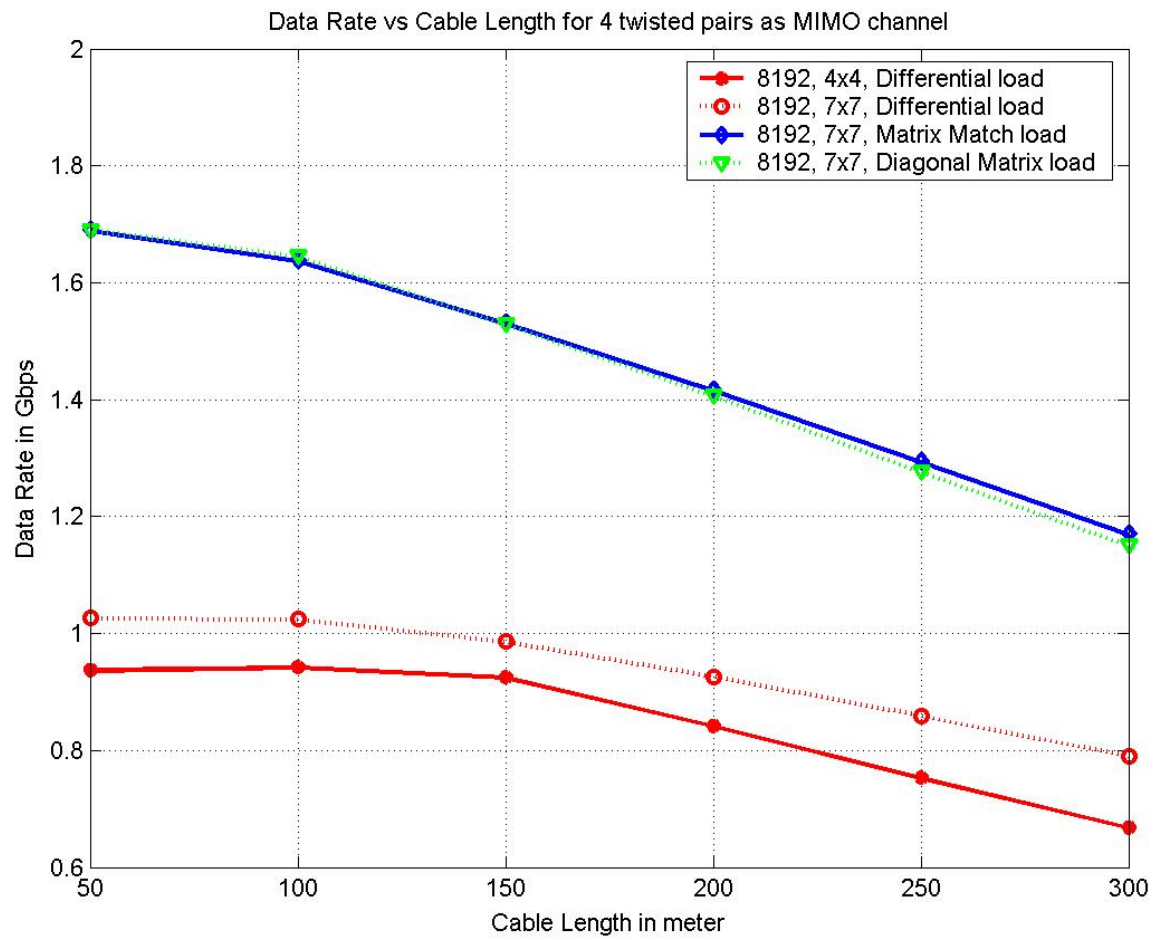


Figure 4, Data Rate vs. Cable Length for 4 Twisted Pairs as MIMO Channel